

- disease (COVID-19)? AJR Am J Roentgenol. 2020;(May):1–5, <http://dx.doi.org/10.2214/AJR.20.23012>.
4. WHO, March 13 Clinical management of severe acute respiratory infection (SARI) when COVID-19 disease is suspected. Interim guidance; 2020.
  5. Xie X, Zhong Z, Zhao W, Zheng C, Wang F, Liu J. Chest CT for Typical 2019-nCoV Pneumonia: Relationship to Negative RT-PCR Testing. Radiology. 2020;296(2):E41–5, <http://dx.doi.org/10.1148/radiol.2020200343>.
  6. Zhao W, Zhong Z, Xie X, Yu Q, Liu J. Relation between chest CT findings and clinical conditions of coronavirus disease (COVID-19) pneumonia: a multicenter study. AJR Am J Roentgenol. 2020;214(5):1072–7, <http://dx.doi.org/10.2214/AJR.20.22976>.
  7. Suo T, Liu X, Feng J, Guo M, Hu W, Guo D, et al. ddPCR: a more accurate tool for SARS-CoV-2 detection in low viral load specimens. Emerg Microbes Infect. 2020;9(1):1259–68, <http://dx.doi.org/10.1080/22221751.2020.1772678>.

Emilio Quaia<sup>a</sup>, Elisa Baratella<sup>b</sup>, Filippo Crimi<sup>a</sup>, Luca Cancian<sup>c</sup>, Paola Crivelli<sup>d</sup>, Andrea Vianello<sup>e,\*</sup>

<sup>a</sup> Department of Radiology, University of Padova, Padova, Italy

<sup>b</sup> Department of Radiology, University of Trieste, Trieste, Italy

<sup>c</sup> Unit of Radiology, Azienda ULSS 6 Euganea, Cittadella, Italy

<sup>d</sup> Unit of Radiology, Department of Clinical and Experimental Medicine, University of Sassari, Sassari, Italy

<sup>e</sup> Respiratory Pathophysiology Division, Department of Cardiac, Thoracic, Vascular Sciences and Public Health, University of Padova, Padova, Italy

\* Corresponding author at: U.O. Fisiopatologia Respiratoria, Azienda Ospedaliera di Padova, Via Giustiniani, 2, 35128 Padova, Italy.

E-mail address: [andrea.vianello@aopd.veneto.it](mailto:andrea.vianello@aopd.veneto.it) (A. Vianello).

4 August 2020

Available online 21 October 2020

<https://doi.org/10.1016/j.pulmoe.2020.10.001>

2531-0437/ © 2020 Sociedade Portuguesa de Pneumologia.

Published by Elsevier España, S.L.U. This is an open access article under the CC BY-NC-ND license (<http://creativecommons.org/licenses/by-nc-nd/4.0/>).

## Reversibility of venous dilatation and parenchymal changes density in Sars-Cov-2 pneumonia: toward the definition of a peculiar pattern



Dear Editor,

In SARS-CoV-2 infection the mild-to-moderate phase of the disease shows type II pneumocytes hyperplasia without hyaline membranes, inflammatory interalveolar infiltrates.<sup>1–4</sup> Vascular changes like hyperplasia/dilatation of alveolar capillaries, new angiogenesis, endothelialitis, thrombotic microangiopathy have been also reported.<sup>3</sup> From a radiologic point of view, Lang et al.<sup>5</sup> using the dual-energy CT scan technology, described peculiar vascular enlargement and mosaic attenuation as a pattern of disordered vasoregulation characterized by a pronounced vascular dilatation (in 85% of the patients) in the affected regions, beside the typical aspects of ground glass attenuation and consolidations. These features were labeled as “hyperemic halo” pattern.<sup>5</sup> Here we describe CT findings of five patients affected by COVID-19 in the early phase of the disease emphasizing the vascular and alveolar changes modified by the gravity.

Five subjects with a diagnosis of COVID-19 based on nasal swab test underwent CT scan in supine and later in the same session the prone position. CT protocol consisted of two consecutive acquisitions respectively in supine and prone position, the latter during administration of contrast medium, with a protocol able to opacify pulmonary both arteries and pulmonary veins.

Clinical and laboratory profiles are summarized in Table 1.

In all the five cases, pulmonary veins were patent. Other radiological features for each patient were as follows:

**Case 1:** 78 years-old male. In the supine position, focal pure ground glass opacities were present in both upper lobes, and some peripheral part-solid ground glass areas with a coexisting crazy paving attenuation in both costophrenic angles. Furthermore, the peripheral branches of the pulmonary veins of the lower lobes appeared enlarged. In the prone position a significant decrease in diameter of veins and a kind of parenchymal ground glass attenuation in both lower lobes. Moreover, a rapid reduction of the density was observed in the “former crazy paving component” that changed into pure ground glass attenuation (Fig. 1).

**Case 2:** 64-year-old male. Subsegmental pulmonary arteries defects were present in the right lower lobe. Pulmonary veins showed a relative reduction in caliber in the prone positioning.

**Case 3:** 52 year old female. Bilateral central and peripheral ground glass attenuation and vessel enlargement. In the right upper lobe and in the left lower lobe the consolidative aspect present in supine position reduced significantly in the prone. Moreover, veins decreased in caliber (Fig. 2).

**Case 4:** 57 years old female. Bilateral, extensive areas of ground glass attenuation with central and peripheral distribution, some peripheral consolidation in upper and lower lobes and bilateral venous enlargement. In the prone position a significant reduction in caliber of the enlarged veins is associated with relative increase in density of the pulmonary infiltrates in the anterior segments of both upper lobes.

**Case 5:** 58 years old female. Part-solid ground glass attenuation in supine position with band-like opacities in left lower lobe. Vessel enlargement was present in both lower lobes, mainly on the left. With the prone positioning the ground glass attenuation redistributed in the medullary portion of the lung, with a concomitant reduction in density attenuation. Caliber of the veins reduced (1.2 vs 2.8 mm).

**Table 1** Clinical and laboratory features.

Clinical features	Patient 1	Patient 2	Patient 3	Patient 4	Patient 5
Age	79	64	52	57	58
Gender	Male	Male	Female	Female	Female
Smoking Habitus	Former smoker	Former smoker	Non-smoker	Nonsmoker	Former smoker
Comorbidity	Hypertension	Multiple sclerosis			Asthma Hypertension
	Psoriasis				
	Diverticulosis				
	Anemia				
Contact epidemiology	Hospital	Family member	Family member	Return from abroad	Family member
BMI	24	20	21	30	32
Symptoms	Fever	Fever	Fever Cough Epigastric pain Diarrea	Fever Headache Dyspnea	Fever Dyspnea
Days of symptoms (n)	5	4	7	7	7
Saturation in room air	96%	97%	97%	86%	96%
Treatment		Interferon*		Azithromycin**	
C reactive protein (mg/L)	79	16.1	47.7	139.2	17.5
LDH (U/L)	305	254	238	487	159
D-Dimer ( $\mu\text{g/mL}$ )	1903	499	663	2245	1369
Ferritin (ng/mL)	138	1677			
IL-6 (pg/mL)	29.8	34.4			
Platelets (n/mm <sup>3</sup> )	63.000	154.000	275.000	228.000	356.000
Lymphocytes (10 <sup>9</sup> /L)	600	1780	1310	1640	1550

The relevant observations of this series are: the enlarged vessels are pulmonary veins; the diameter of these enlarged vessels and the density of ground glass and/or crazy paving areas pouring in them decrease when they are no longer in the dependent zones.

These findings were detected in patients with an early and mild-to moderate form of disease supporting the hypothesis that a large part of the ground glass attenuation/crazy paving pattern could be due to the vascular changes taking place in the alveolar septa instead of accumulation of proteinaceous edema and hyaline membranes in the alveolar spaces.<sup>3</sup>

The "bandlike" opacities described in Covid-19 pneumonia are reversible in the prone position, suggesting again the presence of lung parenchymal vascular gravity-dependent changes.<sup>5</sup>

Furthermore, dilatation of the lumen of the pulmonary veins reversed by pronation could be related to dysregulation of their muscular tone induced by substances produced

in the areas with ground glass/crazy paving opacification and released in the blood flow.<sup>6,7</sup>

The significant increase of oxygen saturation after pronation observed in patients with early stage of COVID-19 interstitial pneumonia might not actually reflect the recruitment of previously atelectatic alveoli, as observed in cases in which interalveolar edema, hyaline membranes and loss of alveolar stability are the histopathologic background, but rather the reduction of the "dead space" and shunt effect related to pulmonary capillary and venous blood redistribution induced mainly by gravity changes.<sup>7</sup>

In conclusion in this series we suggest that intra-alveolar capillary changes could be the main anatomic background of ground glass/crazy paving opacification, and hypothesize a link between veins enlargement, ground glass/crazy paving opacification and the pathophysiology profile observed in the early phase of the disease. We labelled all these features "venoplegic/hyperemic pattern".

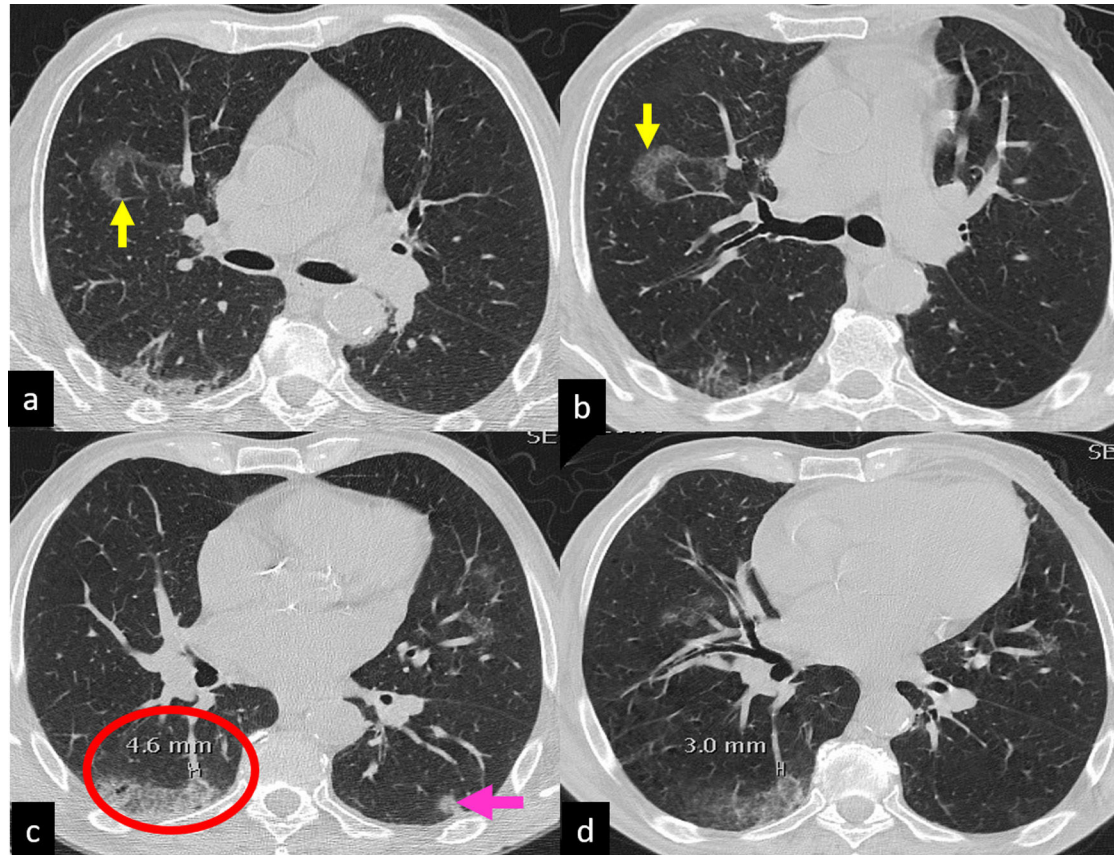


**Figure 1** CT scan in supine (a,c) and prone (b,d) position. Some rounded areas of pure ground glass attenuation are present in the right upper lobe (a, upward yellow arrow), middle lobe and lingula. The GG attenuation in right upper lobe, in prone becomes crazy paving and is associated with occurring of an inside vessel enlargement (b, downward yellow arrow).

In the right lower lobe a part-solid ground glass attenuation with a coexisting minimal crazy paving pattern, is present beneath the pleura (c; red ellipse) in the apical and postero-basal segments.

Some vessel enlargement is present in both lower lobes. In the right lower lobe, the enlargement is both outside and inside the GG attenuation and involves branches of the pulmonary veins (caliber of 4.6 mm). Finally, in the left lower lobe, a nodular consolidation is present, adjacent to the pleura (pink arrow), with a drastic reduction in density with the prone positioning.

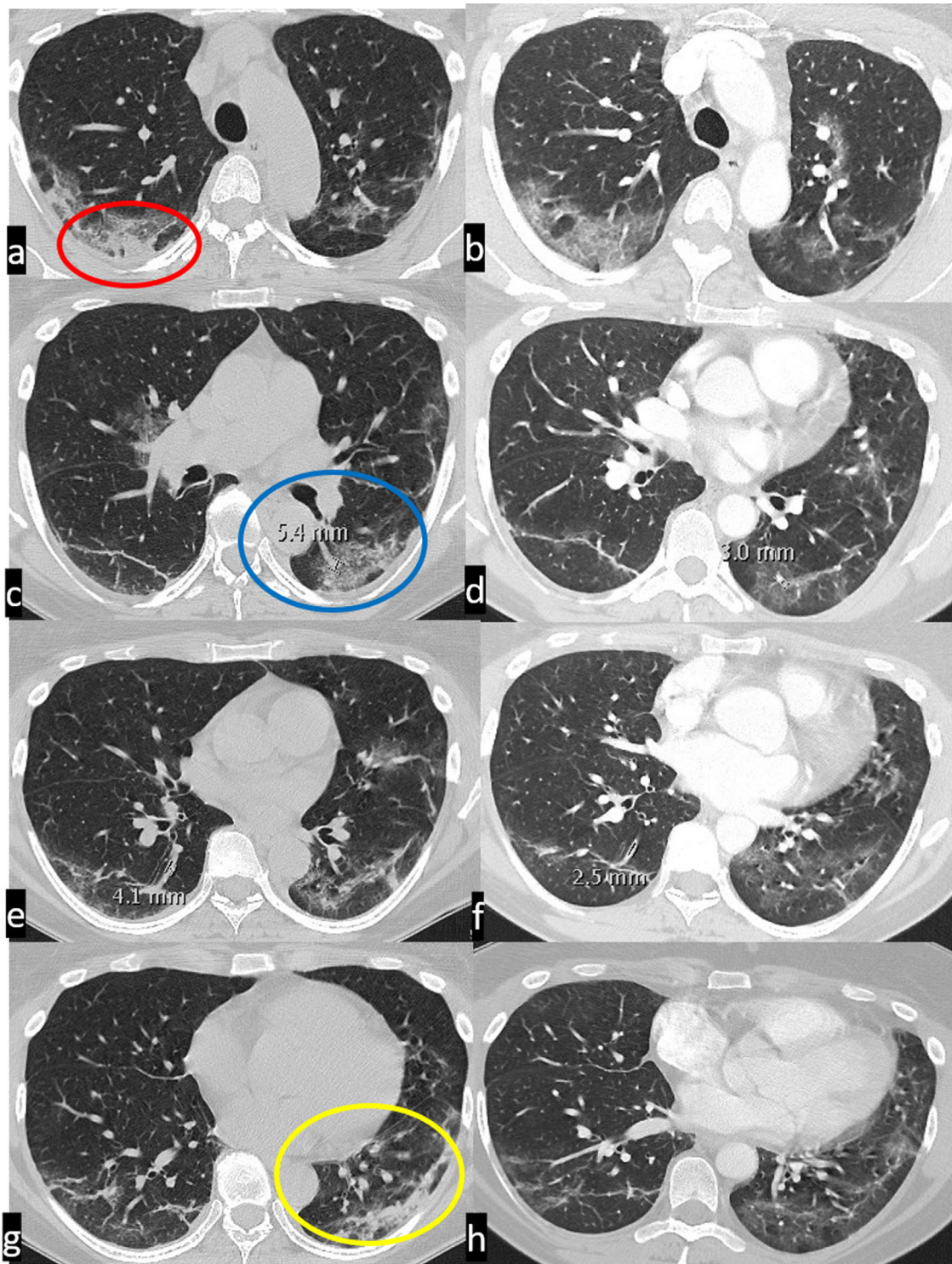


**Figure 2** CT scan in supine (a, c, e, g) and prone (b, d, f, h) position. Bilateral peripheral ground glass attenuation, with solid component in the right postero-basal segment (red ellipse) and left postero-basal segment of the left lower lobe (yellow ellipse). The density of the attenuation decreases significantly with prone positioning. Vessel enlargement, consisting in venous dilatation, is present in both lower lobes, with a significant reduction in caliber with prone positioning (in the left lower lobe: 3 mm vs 5,4 mm).

## Appendix A. Supplementary data

Supplementary material related to this article can be found, in the online version, at doi:<https://doi.org/10.1016/j.pulmoe.2020.10.010>.

## References

1. Tay MZ, Poh CM, Rénia L, MacAry PA, Ng LFP. The trinity of COVID-19: immunity, inflammation and intervention. *Nat Rev Immunol*. 2020;6:363–74.
2. Carsana L, Sonzogni A, Nasr A, Rossi RS, Pellegrinelli A, Zerbi P, et al. Pulmonary post-mortem findings in a series of COVID-19 cases from Northern Italy: a two-Centre descriptive study. *Lancet Infect Dis*. 2020. S1473-3099(20) 30434-30435.
3. Ackermann M, Verleden SE, Kuehnel M, Haverich A, Welte T, Laenger F, et al. Pulmonary Vascular Endothelialitis, Thrombosis, and Angiogenesis in Covid-19. *N Engl J Med*. 2020;383:120–8. Jul 9.
4. Tian S, Hu W, Niu L, Liu H, Xu H, Xiao SY. Pulmonary Pathology of Early-Phase 2019 Novel Coronavirus (COVID-19) Pneumonia in Two Patients With Lung Cancer. *J Thorac Oncol*. 2020;15:700–4.
5. Lang M, Som A, Mendoza DP, Flores EJ, Reid N, Carey D, et al. Hypoxaemia related to COVID-19: vascular and perfusion abnormalities on dual-energy CT. *Lancet Infect Dis*. 2020.
6. Zhao X, Nedvetsky P, Stanchi F, Vion AC, Popp O, Zühlke K, et al. Endothelial PKA activity regulates angiogenesis by limiting autophagy through phosphorylation of ATG16L1. *Elife*. 2019;8.
7. Gattinoni L, Meissner K, Marini JJ. The baby lung and the COVID-19 era. *Intensive Care Med*. 2020;46:1438–40.

S. Piciucchi<sup>a,\*</sup>, C. Ravaglia<sup>b</sup>, A. Vizzuso<sup>a</sup>, M. Bertocco<sup>a</sup>, V. Poletti<sup>b,c</sup>

<sup>a</sup> Department of Radiology, Ospedale GB Morgagni, Forlì, Italy

<sup>b</sup> Department of Diseases of the Thorax, Ospedale GB Morgagni, Forlì, Italy

<sup>c</sup> Department of Respiratory Diseases & Allergy, Aarhus University Hospital, Aarhus, Denmark

\* Corresponding author at: Ospedale GB Morgagni, Via C. Forlanini 34, Forlì, Italy.

E-mail address: [piciucchi.sara@gmail.com](mailto:piciucchi.sara@gmail.com) (S. Piciucchi).

21 September 2020

Available online 16 November 2020

<https://doi.org/10.1016/j.pulmoe.2020.10.010>

2531-0437/ © 2020 Sociedade Portuguesa de Pneumologia.

Published by Elsevier España, S.L.U. This is an open access article under the CC BY-NC-ND license (<http://creativecommons.org/licenses/by-nc-nd/4.0/>).

## Cystic fibrosis and amyotrophic lateral sclerosis, an unexpected association



Dear Editor:

Cystic fibrosis (CF) is a multisystemic disease with clinical heterogeneity, and progressive lung disease remains the major cause of morbidity and mortality.<sup>1</sup> Some CF patients can be diagnosed later in life. Studies have suggested that patients with a delayed diagnosis survive better, reflecting the prevalence of mutations with a less severe phenotype.<sup>2</sup> Some rarer mutations have been associated with mild CF and delayed diagnosis; one such example is the p.Val232Asp mutation.<sup>3</sup>

Amyotrophic lateral sclerosis (ALS) is a progressive neurodegenerative disease that frequently spreads to involve most muscles leading to severe disability.<sup>4,5</sup> Progressive weakness of respiratory muscles leads typically to respiratory failure, and lung function tests are valuable in predicting its course. The decline in pulmonary function closely correlates with death for patients not managed with respiratory aids (non-invasive ventilatory support – NVS, and cough assistance techniques).<sup>6</sup>

A twenty-two years old male, with a history of allergic asthma and rhinitis since childhood, with no current follow-up. No smoking or relevant family history. He presented with weakness of upper right limb, and muscle cramps, for four months. In association, he referred to worsening of cough and sputum. The neurologic examination revealed atrophy of the right forearm and arm, hyperreflexia and weakness

of the upper limbs. Besides the presence of fever, the physical examination was normal. The patient was admitted to the Neurology department for clinical evaluation. Laboratory studies showed a slight elevation of infection markers. Arterial blood gases test were normal. Brain/vertebral magnetic resonance imaging and electromyography (EMG) were normal. Chest computed tomography scan showed cylindrical bronchiectasis with wall thickening, with a tree-in-bud micronodular pattern (Fig. 1, panel A–C). Due to recurrent respiratory infections since childhood, with cough and chronic bronchorrhea and, isolation of methicillin-susceptible *Staphylococcus aureus* in bronchial secretions, CF was suspected. The sweat test was 91 mmol/L, and the genetic study identified p.Val232Asp and p.Phe508del mutations. Both neurological and respiratory symptoms improved with antibiotic therapy, so the patient was discharged. He began follow-up and treatment at the CF outpatient clinic, and radiological improvement was noticeable (Fig. 1 – panel D). No other organ involvement was observed. Spirometry revealed moderate obstructive ventilatory pattern (FVC: 2690 mL/62.9%; FEV1: 2440 mL/65.9%). For the following three months, he experienced worsening of the neurological deficits, with severe weakness of the four limbs (upper right limb with muscle atrophy, Fig. 1 – panel E–F), with an abnormal gait. Repetition of EMG showed neurogenic injury and active denervation, and with the clinical background were indicative of a definitive ALS diagnosis. At this point, he was experiencing a decline in respiratory muscle function, with a VC of 2100 mL, decreasing 15% in the supine position, a peak cough flow of 270 L/min and elevation of partial carbon dioxide pressure (47.8 mmHg). Home mechanical ventilation was initiated with NVS (assisted/controlled